

**EFFECTS OF ELECTRODE MATERIALS ON ELECTRICAL PROPERTIES
OF $\text{CaCu}_3\text{Ti}_4\text{O}_{12}$ AT 100 Hz – 1 GHz**

MUHAMMAD AZWADI BIN SULAIMAN

JULY 2013

DECLARATION

I declare that this thesis is the result of my own research, that it does not incorporate without acknowledgement any material submitted for a degree or diploma in any university that it does not contain any materials previously published, written or produced by another person except where due reference is made in the text.

Signed :

Candidate's Name : Muhammad Azwadi Bin Sulaiman

Dated :

Signed:

Supervisor's Name: Prof. Dr. Zainal Arifin Ahmad

Dated:

**EFFECTS OF ELECTRODE MATERIALS ON ELECTRICAL PROPERTIES
OF $\text{CaCu}_3\text{Ti}_4\text{O}_{12}$ AT 100 Hz – 1 GHz**

by

MUHAMMAD AZWADI BIN SULAIMAN

**Thesis submitted in fulfillment of the requirements
for the degree of
Doctor of Philosophy**

JULY 2013

ACKNOWLEDGEMENT

In the name of Allah, the Most Gracious and the Most Merciful, all praise to Allah for the strength and His blessing to me in completing this thesis, Alhamdulillah.

Firstly, I would like to acknowledge my highly spirited supervisor, Assoc. Prof. Dr. Sabar D. Hutagalung, who has continuously guided me in this study. His invaluable supervision and help throughout the experimental and thesis work have contributed to the success of this research. Special appreciation is given to him on his kindness.

Prof. Dr. Hj. Zainal Arifin Ahmad is my inspiring co-supervisor. He has showed the right route to do the research and constantly motivated me to increase the efforts. Special thanks to him and hopefully he is always given a good health.

I am also infinitely grateful to be awarded PhD Fellowship Scheme by Universiti Sains Malaysia. The scheme has sponsored me to pay the studies fees and funded me with allowances during my studies. I also gratefully acknowledged the Research University Postgraduate Research Grant Scheme (RUPRGS) from Universiti Sains Malaysia under project no. 1001/PBAHAN/8044053 who funded all of researches apparatus, equipment and conference fees.

I expressed my appreciation to the School of Materials and Mineral Resources for the opportunities to gain knowledge in the most established research learning center in this country. The supports from the dean, lecturers and other staffs are not forgotten, especially Mr. Sharul Ami Zainal Abidin, Madam Fong Lee Lee, Mr. Mohd Shahid Abd Jalal, Mr. Mohamad Zaini Saari, Mr. Mohd Farid Abd Rahim, Mr. Abdul Rashid Selamat, Mr. Mokhtar Mohamad, Mr. Mohd Azam Rejab, Mr.

Hasnor and Mrs. Haslina Zulkifli have given me an uncountable help to run this project.

As well as my postgraduate friends from laboratory of 0.36, Nik Akmar, Johari, Fariz, Zahirani, Rashid, Mohd Arif, Najmi, and Wan Fahmi who always give brilliant ideas and problem solving suggestions to me. Hopefully, our friendship lasts forever.

For my beloved wife, Intan Marini and my cute daughter Ayatul Aliya Arifah, special thanks for the understanding efforts and the given sacrifice is very invaluable. Sincere thanks also to my father, mother and siblings for their support, courage, and advice to complete this study.

Finally, all the best to my other companion especially from postgraduate student whose give me the support, idea and suggestion to succeed in my study. Thank you.

Sincerely,

MUHAMMAD AZWADI BIN SULAIMAN

TABLE OF CONTENTS

ACKNOWLEDGEMENTS	ii
TABLE OF CONTENTS	iv
LIST OF TABLES	viii
LIST OF FIGURES	ix
LIST OF APPENDICES	xiii
LIST OF MAIN SYMBOL	xiv
LIST OF PUBLICATIONS	xv
ABSTRAK	xvi
ABSTRACT	xviii
CHAPTER 1: INTRODUCTION	1
1.1 Electroceramic Materials	1
1.2 Problem Statement	4
1.3 Research Objective	5
1.4 Research Approach	6
CHAPTER 2: LITERATURE REVIEW	9
2.1 Introduction	9
2.2 Dielectric Material	9
2.3 Dielectric Constant	10
2.3.1 Electronic Polarization	12
2.3.2 Atomic or Ionic Polarization	13
2.3.3 Orientation Polarization or Spontaneous Polarization	13
2.3.4 Interface or Space Charge Polarization	14
2.4 Miniaturization of Electronic Device	15
2.5 High Dielectric Constant Ceramic	19
2.6 Calcium Copper Titanate ($\text{CaCu}_3\text{Ti}_4\text{O}_{12}$)	21

2.7	Electrode Materials and Surface Layer Effects	23
2.8	Internal Barrier Layer Capacitance (IBLC)	30
2.9	Planar Defect on CCTO Crystal	31
2.10	Processing of CCTO	32
2.10.1	Composition Formulation	33
2.10.2	Mixing	34
2.10.3	Calcination	36
2.10.4	Pressing	38
2.10.5	Sintering	39
2.11	Characterization Technique	42
2.11.1	Particle Size Distribution	43
2.11.2	Thermal Analysis (TA)	43
2.11.3	Phase Identification Using X-Ray Diffraction (XRD)	45
2.11.4	Microstructure Observation Using Scanning Electron Microscope (FESEM)	46
2.11.5	Electrical Properties	47
2.11.5.1	Dielectric Constant and Dielectric loss	49
2.11.5.2	Impedance Complex Plane	51
2.11.5.3	Current-Voltage Characteristic	52
2.11.6	Density and Porosity Test	54
	CHAPTER 3: MATERIALS AND METHODOLOGY	55
3.1	Introduction	55
3.2	Experimental Procedure	55
3.3	Experimental Process	59
3.3.1	Raw Materials Analyses	59

3.3.2	Processing of $\text{CaCu}_3\text{Ti}_4\text{O}_{12}$	59
3.3.2.1	Composition Formulation	61
3.3.2.2	Mixing	61
3.3.2.3	Calcination	62
3.3.2.4	De-agglomeration	62
3.3.2.5	Uniaxial Pressing	63
3.3.2.6	Sintering	64
3.3.3	Electrode Preparation	65
3.3.4	Heat Treatment to the Electrode-Bulk CCTO Contact	66
3.4	Characterization Techniques	67
3.4.1	Particle Size Distribution	68
3.4.2	Thermal Analysis	68
3.4.3	Phase Identification Using X-Ray Diffraction (XRD)	69
3.4.4	Microstructure Observation Using FESEM	70
3.4.5	Density Test	71
3.4.6	Electrical Properties	72
CHAPTER 4: RESULTS AND DISCUSSION		76
4.1	Introduction	76
4.2	Analyses of Starting Materials	76
4.2.1	CaCO_3 Powder	76
4.2.2	CuO Powder	78
4.2.3	TiO_2 Powder	80
4.3	Analyses of Mixed Powder	81
4.4	Part 1: Calcination Profiles	83
4.4.1	Effect of Calcination Temperatures	85

4.4.2	Effect of Soaking Times	90
4.5	Part 2: Sintering Profiles	91
4.5.1	Effect of Sintering Temperatures	92
4.5.2	Effect of Soaking Times	94
4.5.3	Effect of Microstructure to the Electrical Properties	97
4.6	Part 3: Effect of Electrodes	107
4.6.1	Electrode Heat Treatment	107
4.6.2	Electrode Materials	114
CHAPTER 5: CONCLUSION AND RECOMMENDATION		129
5.1	Conclusion	129
5.2	Recommendation for Future Research	130
REFERENCES		131
APPENDIX A		139
APPENDIX B		140
APPENDIX C		141
APPENDIX D		142
APPENDIX E		143
APPENDIX F		144

LIST OF TABLES

Table 2.1:	Types of instrument to measure impedance	48
Table 3.1:	Codes of samples for calcination.....	56
Table 3.2:	Code of samples for sintering.....	57
Table 3.3 :	Codes of sample for electrode heat treated CCTO with Ag Paste.	58
Table 3.4:	Codes of sample with different electrode materials.	58
Table 3.5:	Raw materials, supplier and purity	59
Table 3.6:	Weight of starting materials to prepare a 50 gram batch powder pure CCTO.	61
Table 4.1:	The resistivity of domains (R_d), domain boundaries (R_{db}) and grain boundaries (R_{gb}) of CCTO by using different electrode materials...	125

LIST OF FIGURES

Figure 1.1 :	Flow chart for overall study process of CCTO through solid state preparation.....	7
Figure 2.1:	The relative permittivity (dielectric constant) as function of frequency (Kao, 2004).....	12
Figure 2.2:	Electronic polarization that results from the distortion of an atomic electron cloud by an electric field (Wyatt and Dew-Hughes, 1974). .	12
Figure 2.3:	Ionic polarization that results from the relative displacements of electrically charged ions in response to an electric field (Wyatt and Dew-Hughes, 1974).....	13
Figure 2.4:	Response of permanent electric dipoles (arrows) to an applied electric field, producing orientation polarization (Wyatt and Hughes, 1974).	14
Figure 2.5:	Space charge polarization which is caused by trapped charge at polycrystalline material (Moulson and Herbert, 2003).	15
Figure 2.6:	A parallel-plate capacitor (a) when a vacuum is present and (b) when a dielectric material is present (Callister and Rethwisch, 2007).	16
Figure 2.7:	Simple cubic structure of perovskite (Howard & Kennedy, 1999)	21
Figure 2.8:	Structure of $\text{CaCu}_3\text{Ti}_4\text{O}_{12}$ showing tilted oxygen octahedra. White, light, dark, and black atoms are O, Ca, Cu, and Ti respectively. Dashed lines indicate 40-atom primitive cell of antiferromagnetic spin structure (He et al., 2002).....	23
Figure 2.9 :	Energy level diagram for an ohmic contact between a metal and an n-type semiconductor (Kao, 2004).	25
Figure 2.10:	Energy level diagrams for a contact between a metal and an n-type semiconductor (a) before contact, (b) in thermal equilibrium, (c) in intimate contact, and (d) charge density distribution and contact potential (Kao, 2004).....	26
Figure 2.11:	Current–voltage characteristic for a metal–semiconductor rectifying junction.....	27
Figure 2.12:	Current-voltage characteristic for back-to-back Schottky barriers. ...	28
Figure 2.13:	The grain and grain boundary structure model (Moulson and Herbert, 2003).....	30
Figure 2.14:	Equivalent circuit of parallel (Moulson and Herbert, 2003).	31
Figure 2.15:	The particles arrangement in two dimension compound (Reed, 1989).	35

Figure 2.16:	Schematic of solid-state reaction in mixed powders (Rahaman, 2003).	37
Figure 2.17:	Necking formation between spheres as a result of sintering process (German, 1991).....	41
Figure 2.18:	(a) Final stage (b) intermediate stage (c) final stage and (d) finished product (Rahaman, 2003).	42
Figure 2.19:	Polar coordinates and rectangular of the impedance Z plot (Barsoukov and Macdonald, 2005).	49
Figure 2.20:	The current–voltage characteristics of a p–n junction for forward and reverse biases (Callister and Rethwisch, 2007).	53
Figure 3.1:	Sintering profile for temperature and soaking time range.....	64
Figure 3.2:	Edge effect.....	73
Figure 3.3:	Schematic of current-voltage measurement.	75
Figure 4.1:	FESEM micrograph of CaCO ₃ (The micrograph is 5000 of magnification)	77
Figure 4.2:	Particle size distribution of CaCO ₃ powder.....	77
Figure 4.3:	X-ray diffraction pattern of CaCO ₃ powder compared with ICDD 047- 1743.	78
Figure 4.4:	FESEM micrograph of CuO (The magnification of the micrograph is 30.00 × 10 ³).	78
Figure 4.5:	Particle size distribution of CuO powder.	79
Figure 4.6:	XRD pattern of CuO powder compared with ICDD 44-0706.....	79
Figure 4.7:	FESEM micrograph of TiO ₂	80
Figure 4.8:	Particle size distribution of TiO ₂ powder.	81
Figure 4.9:	XRD pattern of TiO ₂ powder compared to ICDD 089-4921.	81
Figure 4.10:	TGA and DTA of starting materials mixture.	83
Figure 4.11:	X-ray diffraction pattern of pure CCTO calcination from 900 to 1000 °C.	85
Figure 4.12:	Lattice parameters of calcined powder of CCTO at different temperature and soaking time.....	86
Figure 4.13:	Crystallite size of calcined powder of CCTO at different temperature and soaking time.....	87

Figure 4.14:	FESEM of calcined powder at different temperature profile.	89
Figure 4.15:	XRD of sintered pellets at different temperature and soaking time. ..	91
Figure 4.16:	Lattice parameters of different sintering temperature and soaking time	92
Figure 4.17:	Crystallite size of different sintering temperature and soaking time..	93
Figure 4.18:	FESEM of pellets surface for normal grain growth.	95
Figure 4.19:	FESEM of pellets surface for abnormal grain growth.....	96
Figure 4.20:	Dielectric constant of sintered pellets at different sintering temperature and soaking time.....	98
Figure 4.21:	Dielectric constant and dielectric loss of different sintering temperature and soaking time of CCTO pellets at frequency a) 1 MHz, b) 10 MHz, c) 100 MHz, and d) 500 MHz.	100
Figure 4.22:	Dielectric loss of sintered pellets at different sintering temperature and soaking time.....	102
Figure 4.23:	The relative density, apparent porosity of sintered CCTO at different temperature and soaking time.....	103
Figure 4.24:	Impedance complex plane of CCTO at different sintering temperature and soaking time.....	104
Figure 4.25:	Schematic impedance complex plane plot for two curves (a) and its equivalence RC circuit (b).....	105
Figure 4.26:	Current-voltage characteristic for CCTO sample sintered at different temperature and soaking time.....	106
Figure 4.27:	Dielectric constant of untreated and treated CCTO (200, 250, 300, 350 and 400°C) measured at low frequency (100 Hz to 1 MHz).....	108
Figure 4.28:	Dielectric constant of untreated and heat treated CCTO (200, 250, 300, 350 and 400°C) measured at high frequency (1 MHz to 1 GHz).	109
Figure 4.29:	Dielectric loss of untreated and heat treated CCTO (200, 250, 300, 350 and 400°C) measured at low frequency (100 Hz to 1 MHz).....	110
Figure 4.30:	Dielectric loss of unheated and heat treated CCTO (200, 250, 300, 350 and 400°C) measured at high frequency (1 MHz to 1 GHz).....	111
Figure 4.31:	Impedance complex plane of untreated and treated CCTO (200, 250, 300, 350 and 400°C) measured at low frequency (100 Hz to 1 MHz).	112

Figure 4.32:	High frequency impedance complex plane of heat treated electrode.	113
Figure 4.33:	Current-voltage characteristic of the sample with different electrode materials.	115
Figure 4.34:	Dielectric constant of CCTO pellets with different electrode materials measured at low frequency.	116
Figure 4.35:	Dielectric constant of CCTO pellets with different electrode materials measured at high frequency.	117
Figure 4.36:	Dielectric loss of CCTO pellets with different electrode materials measured at low frequency.	118
Figure 4.37:	Dielectric loss of CCTO pellets with different electrode materials measured at high frequency.	119
Figure 4.38:	Bulk electrical resistivity of CCTO pellets with different electrode materials measured at low frequency.	120
Figure 4.39:	Bulk resistivity of CCTO pellets with different electrode materials measured at high frequency.	121
Figure 4.40:	Impedance complex plane of CCTO pellets with different electrode materials measured at low frequency, a) wide scale and b) narrow scale.	122
Figure 4.41:	Impedance complex plane of CCTO pellets with different electrode materials measured at high frequency.	123
Figure 4.42:	Frequency dependence of imaginary part (M'') of electric modulus of CCTO pellets with different electrode material measured at high frequency	123
Figure 4.43:	EDX analysis at the silver electrode of CCTO pellet.	127
Figure 4.44:	EDX analysis at the CCTO bulk with silver electrode.	127
Figure 4.45:	EDX analysis at the aluminium electrode of CCTO pellet.	127
Figure 4.46:	EDX analysis at the CCTO bulk with aluminium electrode.	128
Figure 4.47:	EDX analysis at the silver paste electrode of CCTO pellet.	128
Figure 4.48:	EDX analysis at the CCTO bulk with silver paste electrode.	128

LIST OF APPENDICES

- APPENDIX A : The ICSD of $\text{CaCu}_3\text{Ti}_4\text{O}_{12}$ Pattern 01-075-2188
- APPENDIX B : Calculation on Starting Materials Needed to Prepare
A Batch of 50 gram $\text{CaCu}_3\text{Ti}_4\text{O}_{12}$
- APPENDIX C : The ICSD Pattern of CaCO_3 (00-047-1743)
- APPENDIX D : The ICSD Pattern of CuO (00-044-0706)
- APPENDIX E : The ICSD Pattern of TiO_2 (01-089-4921)
- APPENDIX F : The bulk density, relative density and apparent porosity of
the sintered CCTO at different temperatures and soaking
times

LIST OF MAIN SYMBOL

%	Percentage
°	Degree
°C	Degree Celcius
°C/min	Degree Celcius per minutes
J	Joule
MPa	Mega Pascal
GPa	Giga Pascal
mg	milligram
g	Gram
nm	Nanometer
µm	Micrometer
mm	Milimeter
cm	Centimeter
m	Meter
wt %	Weight percent
λ	Wave length
s	second
min	minutes
ε	permittivity
tan δ	tangent lost or dissipation factor
mol%	mole percent
XRD	X-ray diffraction
IS	Impedance Spectroscopy
IBLC	Internal boundary layer capacitance

LIST OF PUBLICATIONS

- Sulaiman, M.A., Hutagalung, S.D., Ahmad, Z.A., 2012. Nanoscale Investigation of Nb-Doped $\text{CaCu}_3\text{Ti}_4\text{O}_{12}$ Grains. *Advanced Materials Research* 364, 455–459.
- Sulaiman, M.A., Hutagalung, S.D., Ain, M.F., Ahmad, Z.A., 2010. Dielectric properties of Nb-doped $\text{CaCu}_3\text{Ti}_4\text{O}_{12}$ electroceramics measured at high frequencies. *Journal of Alloys and Compounds* 493, 486–492.
- Sulaiman, M.A., Hutagalung, S.D., Mohamed, J.J., Ahmad, Z.A., Ain, M.F., Ismail, B., 2011. High frequency response to the impedance complex properties of Nb-doped $\text{CaCu}_3\text{Ti}_4\text{O}_{12}$ electroceramics. *Journal of Alloys and Compounds* 509, 5701–5707.
- Sulaiman, M.A., Hutagalung, S.D., Ahmad, Z.A., Ain, M.F., 2013. Investigation of Grain Size Effect on the Impedance of $\text{CaCu}_3\text{Ti}_4\text{O}_{12}$ From 100 Hz to 1 GHz of Frequency. *Advanced Materials Research* 620, 230–235.
- Sulaiman, MA, Hutagalung, S.D. & Ahmad, ZA. Heat Treatment Effect with the Electrode Contact Of $\text{CaCu}_3\text{Ti}_4\text{O}_{12}$. *Nuclear Science, Technology & Engineering Conference* 2012.

KESAN BAHAN-BAHAN ELEKTROD KE ATAS SIFAT-SIFAT ELEKTRIK CaCu₃Ti₄O₁₂ PADA 100 Hz – 1 GHz

ABSTRAK

CaCu₃Ti₄O₁₂ (CCTO) telah menarik perhatian ramai kerana mempunyai pemalar dielektrik tinggi sehingga 10^5 pada suhu bilik dan tekal dalam julat suhu 100 K hingga 400 K. Pemalar dielektrik tinggi ini menawarkan pengecilan saiz peranti elektronik yang sedia ada. Walaubagaimanapun, CCTO juga memiliki lesapan dielektrik tinggi yang tidak dikehendaki dalam aplikasi elektronik. Untuk mengurangkan lesapan dielektrik, perlu untuk memahami punca respon polarisasi dan mekanisme santaian pada CCTO. Menggunakan pengukuran spektroskopi impedans (IS) pada frekuensi luas 100 Hz hingga 1 GHz, punca kesan polarisasi boleh ditemui. Salah satu punca penting ialah penggunaan berlainan elektrod yang menentukan keadaan sentuhan terhadap jasad CCTO. Penyelidikan ini dijalankan untuk mengkaji kesan bahan elektrod terhadap sifat elektrik CCTO pada frekuensi 100 Hz hingga 1 GHz. Sampel telah disediakan melalui kaedah tindakbalas keadaan pepejal dan bahan mentah daripada CaCO₃, CuO dan TiO₂ telah digunakan. Selepas pencirian, bahan mentah dicampur selama 1 jam dan analisis terma (TGA dan DTA) telah dilakukan. Campuran serbuk dikalsin pada suhu 900 hingga 1000°C selama 3 hingga 6 jam. Analisis fasa (XRD) dan pemerhatian mikrostruktur (FESEM) telah dijalankan. Sampel dikalsin pada suhu 1000°C selama 3 jam menghasilkan fasa CCTO yang hampir tunggal. Serbuk kalsin telah ditekan ke dalam bentuk pelet dan proses pensinteran telah dilakukan antara 1000 hingga 1050°C selama 3 hingga 10 jam. Pensinteran pada 1030°C dan ke bawah menyebabkan puncak XRD beralih ke kiri dan tempoh rendaman 10 jam pada suhu 1040°C telah mengalih puncak XRD ke kanan. Tempoh rendaman yang lebih lama meningkatkan saiz kristal dan tempoh

rendaman selama 6 jam menghasilkan butir yang besar ($> 100\mu\text{m}$). IS melaporkan pemalar dielektrik dan lesapan dielektrik juga meningkat dengan peningkatan tempoh rendaman semasa proses pensinteran. Sataian puncak pada 10 MHz dicadangkan berpunca daripada kehilangan kesan polarisasi pada sempadan butir. Lengkung graf pada pengukuran satah impedan kompleks dimodelkan melalui analisis litar setara berkait dengan kerintangan domain dan sempadan domain. Pencirian voltan-arus yang tidak linear membuktikan halangan Schottky pada CCTO. Sampel yang disinter pada suhu 1040°C selama 4 jam mempunyai pemalar dielektrik yang tinggi dan stabil serta lesapan dielectric yang rendah. Kajian rawatan haba terhadap elektrod dari suhu bilik ke 400°C dalam gas argon mendedahkan peningkatan pemalar dielektrik dengan peningkatan suhu rawatan. Peningkatan pemalar dielektrik ini adalah disebabkan pembentukan halangan Schottky selepas rawatan. Rawatan pada 300°C adalah suhu yang paling sesuai untuk menghasilkan pemalar dielektrik CCTO yang tinggi dengan kehilangan dielektrik rendah. Kesan Schottky terhadap sentuhan telah diperhatikan dengan menggunakan bahan elektrod yang berbeza seperti emas, platinum, perak dan aluminium. Pencirian arus-voltan menunjukkan ciri-ciri bukan linear pada sampel berelektrod platinum dan emas. Ini adalah kerana kedua-dua elektrod mempunyai fungsi kerja yang lebih tinggi daripada elektrod lain. Emas menunjukkan pemalar dielektrik yang tinggi pada 1 MHz (4,398) dan lesapan dielektrik yang baik (0.03 pada 1.58 kHz). Pengukuran sifat elektrik pada julat frekuensi lebar menunjukkan respons dari butir, sempadan butir, domain dan sempadan domain melalui kaedah padanan lengkung satah impedans kompleks. Kerintangan kawasan tersebut telah berubah dengan parameter kajian dan respon pada frekuensi tinggi ialah berkaitan dengan sempadan domain dan telah dimodelkan mengikut analisis litar setara.

EFFECTS OF ELECTRODE MATERIALS ON ELECTRICAL PROPERTIES OF $\text{CaCu}_3\text{Ti}_4\text{O}_{12}$ AT 100 Hz – 1 GHz

ABSTRACT

$\text{CaCu}_3\text{Ti}_4\text{O}_{12}$ (CCTO) has attracted much interest because of its extraordinary high dielectric constant of 100,000 at room temperature and very small temperature dependence in a broad temperature range from 100 K to near 400 K. This high dielectric constant offers opportunities in miniaturization of electronic application nowadays. However, CCTO also possesses high dielectric loss which is undesirable in electronic applications. To lower the dielectric loss, it is necessary to understand the origin of polarization responds and relaxation mechanism in CCTO. Using wide frequency impedance spectroscopy (IS) from 100 Hz to 1 GHz, the origins of polarization effect can be revealed. One of the important origins is the used of different electrode materials which determine the contact condition to the bulk CCTO. A research was carried out to study the effect of electrode materials to the electrical properties of CCTO at the frequencies of 100 Hz to 1 GHz. Samples were prepared through solid state reaction methods and starting materials of CaCO_3 , CuO and TiO_2 has been used. After the characterization, the starting materials were mixed for 1 hour and thermal analysis was done. Mixed powder was calcined at 900 to 1000°C for 3 to 6 hours. Phase analyses and microstructure observation was carried out. Calcination at 1000°C for 3 hours produced almost single phase of CCTO. The calcined powder was pressed into pellet forms and the sintering processes were done between 1000 to 1050°C for 3 to 10 hours. X-ray diffraction (XRD) analysis indicated that sintering at 1030°C and below increased the lattice parameter and long soaking time until 10 hours at 1040°C has decreased the lattice parameter. Longer soaking times are also increasing the crystallite size and 6 hours of soaking time or

more produced large grains ($>100\mu\text{m}$). The IS reported the dielectric constants and dielectric loss are also increased with the sintering soaking time. Relaxation peak at 10 MHz is suggested due to the loss of grain boundaries polarization effects. High frequency curve of impedance complex was observed and modeled as domain and domain boundary contribution in equivalence circuit analyses. The current-voltage characteristic reported the non-linearity and proved the Schottky's barrier of CCTO. Sample sintered at 1040°C for 4 hours have stable and high dielectric constant and low dielectric loss over the frequency range. Heat treatment study to the electrode from room temperature to 400°C in argon gas revealed the increase of dielectric constant with the increasing of treatment temperature. The dielectric constant improvement was due to more Schottkys contact formation after the treatment. Treatment at 300°C is the most suitable temperature to produce high dielectric constant CCTO with low dielectric loss. Schottky's effect to the contact were observed by applying different electrode material, gold, platinum, silver and aluminium and non-linear of current-voltage characteristic was revealed on Pt and Au electrode. This is due to both electrodes have higher work function than the other electrodes. Samples with Au electrode showed high dielectric constant at 1 MHz (4,398) and low dielectric loss (0.03 at 1.58 kHz). Wide frequency measurement of the electrical properties shows the responds from grain, grain boundary, domain and domain boundary through impedance complex plane curve fitting method. Their resistivities have changed with the study parameters and high frequency respond associated with domain boundary resistivities has been modelled according the equivalence circuit analysis.

CHAPTER 1

INTRODUCTION

1.1 Electroceramic Materials

One of the most studied advanced ceramics is electroceramic. The term electroceramic is used to explain ceramics materials that have been formulated for certain function by designing their electrical, magnetic or optical properties. These properties can be modified or designed by controlling their processing, microstructure or doping in order to produce device with specific properties. Electrical properties are the most desired properties of electroceramic such as resistivity, conductivity, dielectric constant, dielectric loss, dielectric strength and capacitance (Moulson and Herbert, 2003).

The used of electroceramics in the electronic industries is mostly based on its dielectric properties. Electroceramic especially from titanate-based have very high dielectric constant and mostly exceeded 1,000 at 1 MHz and below. This increasing of dielectric constant can decrease the size of electronic devices (Banerjee and Krupanidhi, 2011; Ni and Chen, 2009; Yu et al., 2008). Therefore current market growth of mobile and portable devices caused an increasing demand to electroceramic on miniaturization of many electronic components such as capacitor, resonator, resistor and oscillator. Some of the titanate-based electroceramics have attracted many researchers to study and improve the performance of materials especially on BaTiO_2 (BT), BaSrTiO_2 (BST) and the latest finding is $\text{CaCu}_3\text{Ti}_4\text{O}_{12}$ (CCTO) (Callister and Rethwisch, 2007; Lin et al., 2008).

According to Ye, (2008), BT and BST have become well established as the preferred high dielectric materials for electronics devices since year 1958. The

dielectric constant of BT and BST can achieve 5,000 and 10,000, respectively. The materials have been commercialized and applied in current electronic devices in the markets. The researches on higher dielectric constant material other than BST which is limited to 10,000 are on-going process to fulfil the miniaturization purpose for future electronic device.

A relatively new high dielectric constant material, CCTO was initially synthesized by Bochu et al., (1979). Bochu et al., (1979) have reported the crystal structure of CCTO in 1979 and the giant dielectric constant was observed by Subramanian et al., (2000). CCTO possesses a very high dielectric constant of 100,000 at room temperature and very small temperature dependence in a broad temperature range from 100K to near 400K (Ramirez et al., 2000; Subramanian et al., 2000). These extraordinary properties have attracted much interest from researchers to identify the nature of the high dielectric constant. Furthermore, the dielectric constant of CCTO is almost frequency independent below 10^6 Hz, which is desirable to replace current electroceramic for many microelectronics applications (Homes et al., 2001).

However, the dielectric loss of CCTO is still slightly high for commercial applications. The high dielectric loss is undesirable properties because of dissipation of energy (Jumpatam et al., 2012). The dielectric loss of CCTO ceramics is about ~ 0.1 at 1 kHz at room temperature (Mu et al., 2009). It is necessary to understand the origin of dielectric loss in CCTO ceramics to find an effective method to lower it (Masingboon et al., 2007, Homes et al., 2003 and Marques et al., 2006). This understanding will help the processing of CCTO in order to design certain electrical properties such as dielectric constant of 10,000 at 1 MHz with dielectric loss of 0.07.

One of the important origins is the used of different electrode materials (Lunkenheimer et al., 2004).

Gold, platinum, silver and aluminium have high electrical conductivity and possibly used as electrodes. Electrodes connect the bulk of ceramics to the circuit wire in order to observe their electrical respond. The electrical respond is either under frequency domain or direct current. Most recent equipment such as impedance spectroscopy (IS) is capable to observe from 1 MHz to 1 GHz range of electrical responds. The high conductive metal electrode is always used to connect this equipment to the testing samples. The contact between the electrode and ceramics surface speculated created Schottky barrier layer effect which produce metal-semiconductor junction with depleting region created in the ceramics surface (Deng et al., 2009). The region increased the capacitance and results in high dielectric constant of CCTO.

Interface layer of depleting region between electrode and bulk CCTO were suggested by many researchers as the origin of high dielectric constant of CCTO (Lunkenheimer et al., 2002; B. Shri Prakash and Varma, 2007; Putjuso et al., 2011; Wang and Zhang, 2006; Yang et al., 2005). They also studied different electrode materials in order to identify on how the electrical properties are influenced.

But most of them studied the effects of electrode materials on the CCTO from low frequency to medium frequency window. The range of frequency is enough to observe the contact effect to the electrode/bulk CCTO but in order to observe the contact effect to the grains and grains boundaries or domains and domain boundaries, higher frequency measurement is necessary. Frequency respond of the origins of

high dielectric constant can be observed by using impedance spectroscopy in form of impedance complex plane or cole-cole plot. Electrical impedance complex planes below 10 MHz are consisting one curves only (Amaral et al., 2010a; Sinclair et al., 2002) and this incapable to differentiate the electrode materials effects with other effect like grain boundary effect.

In this study, the electrical properties of CCTO were investigated from low to high frequency range using different electrode materials. Heat treatments to the electrode were also done in order to optimize the contact between the electrodes and ceramic surface.

1.2 Problem Statement

The Schottky barrier layer formed between sample and electrode will affects the electrical properties of sample. In CCTO, this effect has been investigated at low frequency (1 Hz – 1 kHz) (Adams et al., 2006; He et al., 2009) as well as at medium frequency (1 kHz – 1 MHz) (L. Liu et al., 2009). Wide frequency range study from low until high frequency (100 Hz to 1 GHz) is not widely reported yet.

The most popular technique to investigate contact effect is by using impedance complex plane or cole-cole plot through curve fitting technique. However, only a few researchers investigated the impedance complex plane of CCTO until mid-frequency range (till 110 MHz) and found an incomplete curve at the high frequency region of the cole-cole plot (L. Liu et al., 2009; Shao et al., 2007). As the result, the incomplete curve cannot give sufficient point of reading to draw curve fitting in order to estimate the resistance of the contributed element.

To resolve this problem, wider frequency range of measurement (till to GHz range) should be able to complete the point of reading to draw cole-cole plot and identify all of the origins of the high frequency curve for CCTO impedance. Some researches succeeded to observe the curve by cooling the samples to increase electrical resistivity (Shri Prakash and Varma, 2006). In this study, the wide range of frequency measurement is used to reveal the curves and identifies all of the origins at room temperature.

The study of the origins of electrical responds of CCTO including electrode materials effect is very important in order to understand many electrical properties of CCTO such as dielectric constant, dielectric loss and resistivity. This will address the cause of dissimilarity from previous researcher reports on CCTO electrical properties. Internal boundary layer capacitance (IBLC) model indicated that insulative grain boundary layers with semi conductive grains forms space charge polarization and caused the high dielectric constant of CCTO. This model were widely accepted as the origins of the very high-K of CCTO. But the model fails to explain the high dielectric constant of single crystal and thin films of CCTO. New model should be investigated and proposed based on the other origins of CCTO electrical properties and not only the IBLC effect on the grain boundary layer.

1.3 Research Objectives

1. To investigate heat treatment effect to the Ag paste contact of CCTO bulk and the properties of CCTO synthesized via solid state reaction method.
2. To investigate contact of different electrode materials and effect to the properties of CCTO at wide frequency range (100 Hz to 1 GHz).

3. To propose a model of the origin of the high dielectric constant of CCTO.

1.4 Research Approach

Figure 1.1 shows flow chart of the overall process on this study. Preparation process of CCTO was through solid state reaction and based on previous experimental done by Homes et al., (2001). They investigated on the charge transfer phenomena inside of high dielectric constant material CCTO and $\text{CdCu}_3\text{Ti}_4\text{O}_{12}$.

Firstly, the starting materials were characterized to identify the distribution of particle size, morphology and the phase present. The properties of the raw material also affected the end product properties. The raw materials were weighted according to stoichiometry ratio. The mass for mixing each of them was specific to the mole of CaCO_3 , CuO and TiO_2 . Mole ratio for CaCO_3 : CuO : TiO_2 is 1:3:4. The raw materials were mixed using ball milling for 1 hour by using alumina jar. Zirconia balls were used as grinding media with mass ratio to the raw materials is 10:1 and 50 ml of ethanol assisted the mixing process. Ethanol is used as a wetting agent for the mixing and can be easily removed during the drying process.

Thermogravimetry (TGA) and Differential Thermal Analysis (DTA) were used to identify reaction behaviour of the mixed powder for calcination study. Based on the TGA and DTA data, the mixed powders were calcined from temperature 900 to 1000°C from 3 to 6 hours. The calcined powder was characterized for their phases present, and the microstructure was determined. From the XRD analysis, sample calcined at 1000°C for 3 hours have formed CCTO with the lowest secondary phases of constituent material and this calcination profile was selected as an optimized

parameter for further process. Then the optimized calcined powder was pressed into pellets formed using hydraulic press at 300 MPa for sintering process.

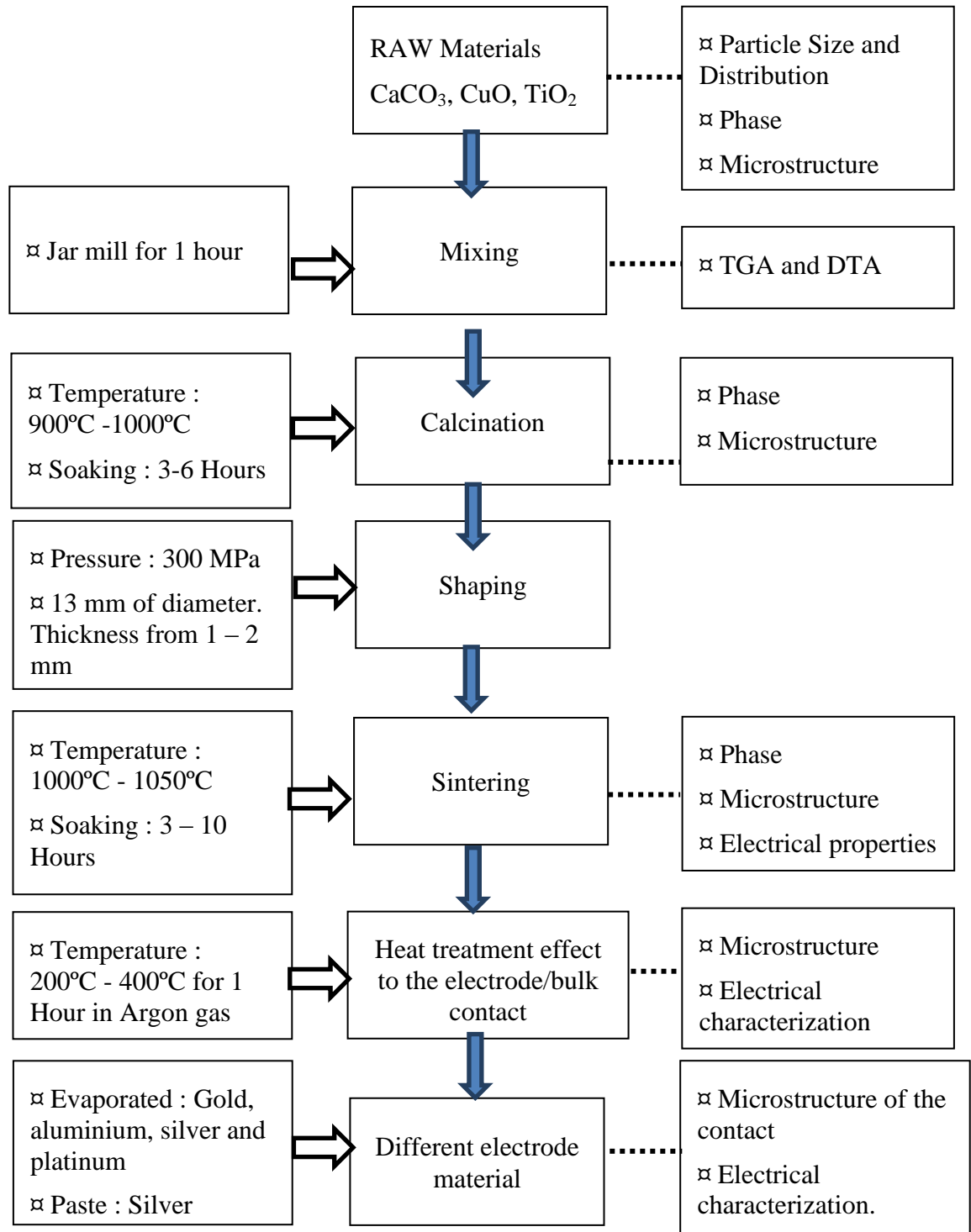


Figure 1.1 : Flow chart for overall study process of CCTO through solid state preparation.

Sintering process was varied from 1000 to 1050°C to consolidate the green body. After sintering process, the pellets are characterized for their density, dielectric constant, dielectric loss, microstructure and phase analysis. Samples sintered at 1040°C for 4 hours were selected as the best sample for further characterization.

Electrode preparation was started by grinding and polishing the pellets sample and silver paste was used as a standard electrode. Heat treatment of silver electrode was done in argon environment in order to investigate the electrode contact effect. The treatment temperature was varied from 200 to 400°C for an hour. The treatment temperature was limited to 400°C because sample showed increasing dielectric loss when treated at 350 and 400°C. After the characterization of their electrical properties and the microstructure of the contact to the bulk CCTO, the heat treated samples at 300°C was selected as the best sample.

Different electrode materials were applied to investigate their effect to the properties of CCTO. Gold, aluminium, platinum and silver were evaporated by thermal evaporator and silver paste also was applied. Samples were characterized to quantify their properties and gold was selected as the best electrode materials.

CHAPTER 2

LITERATURE REVIEW

2.1 Introduction

Electroceramics are special formulated, high purity ceramic compound to function as electrical, magnetic or optical circuit applications. Because of wide range of electrical properties capabilities, electroceramics were categorized according to their properties, which are piezoelectric, pyroelectric, ferroelectric, semiconductor, electro-optic, dielectric, magnetic and superconductors. One of the most popular electroceramics is dielectric material. Dielectric materials with high electrical resistivity are the most important application in electric and electronic industries. Their dielectric constant or real permittivity (ϵ') and dielectric loss ($\tan \delta$) play a major factor to define the performance for certain application. Increasing the dielectric constant properties of the ceramics can scale down many electronic devices such as capacitor, resonator, resistor and oscillator (Kao, 2004; Ye, 2008).

2.2 Dielectric Materials

Dielectric materials basically are resistive ceramics capable of preventing electrical flow. The ability to flow electricity can be described using conduction band and valence band of the materials. The overlap of these bands always happen to the metals or conductor and the ceramics or polymers usually show the gap between the valence and the conduction band and caused materials to prohibit flow of electricity otherwise the condition of materials was changed and the bands become overlap such as by excitation of the valence band (Moulson and Herbert, 2003).

Dielectric material influence polarization phenomena either from as intrinsic or extrinsic elements when the electric potential was applied. Intrinsic element that

contributing to the polarization may come from crystal structure of the materials and extrinsic element of materials such as microstructure can form the sources of polarization. This property is defined as dielectric property which is proportion of the amount of polarization elements inside the dielectric material. When dielectric material are placed in an electric field, the electrons and protons of its constituent atoms reorient themselves as a respond to the field and in some cases polar molecules become polarized. As a result of this polarization, the atoms or molecules are under stress and they store energy that becomes available when the electric field is removed. The higher total polarizations caused higher capability of the ceramic to hold the energy. This total polarization inside of dielectric material is measured as dielectric constant (Kao, 2004).

2.3 Dielectric Constant

Dielectric constant or also known as relative permittivity is the ratio of the material permittivity and permittivity to vacuum. Dielectric constant is an indicator of the total net polarizations effect of the dielectric materials to the electrical field. The dielectric constant is independent to the material geometry, size and shape. Most of the dielectric material also show dielectric constant of independent to the electric field strength for below certain critical field or above otherwise carrier injection will take apart and become dominant (Kao, 2004). The frequency of applied electrical field strongly affected the dielectric constant as well as the chemical structure, temperature, pressure and dopant as the major factors (Kao, 2004). Basically, the dielectric constant is related to attraction and repulsion of bounded electric charges inside the dielectric material bulk. The attraction and repulsion responds to the force to reduce the potential energy of the whole electrically stressed system to a minimum state. This attraction and repulsion can be also described as polarization phenomena

which were studied and reported in many literatures (Carter and Norton, 2007; Kao, 2004; Moulson and Herbert, 2003; Phillippe and Jean-Claude, 2007; Rahaman, 2003). Four basics types of electric polarization found on dielectric material were proposed and is not necessary contained in all of them in a single dielectric materials.

- a. Electronic polarization
- b. Atomic or ionic polarization
- c. Orientation or spontaneous polarization
- d. Interface or space charge polarization.

Fig. 2.1 shows example of dielectric constant as function of frequency. The dielectric constant decreases with the increasing frequency due to the constituent types of polarizations start to became insignificant at the different frequency range. In region A, the polarization is due completely to electron polarization. In region B, it is due to the combination of electronic and atomic polarization, and so on.

Each type of polarization reorients their dipole according to the AC electrical field. The orientation process requires some finite of time and different time to each of the polarization type which depend on capability of particular dipoles to realign. The different of time causes the variation of dielectric constant at a specific frequency. Basically at higher frequency, some of the polarization types do not have enough time to reorient and loss the contribution to dielectric constant of the materials.

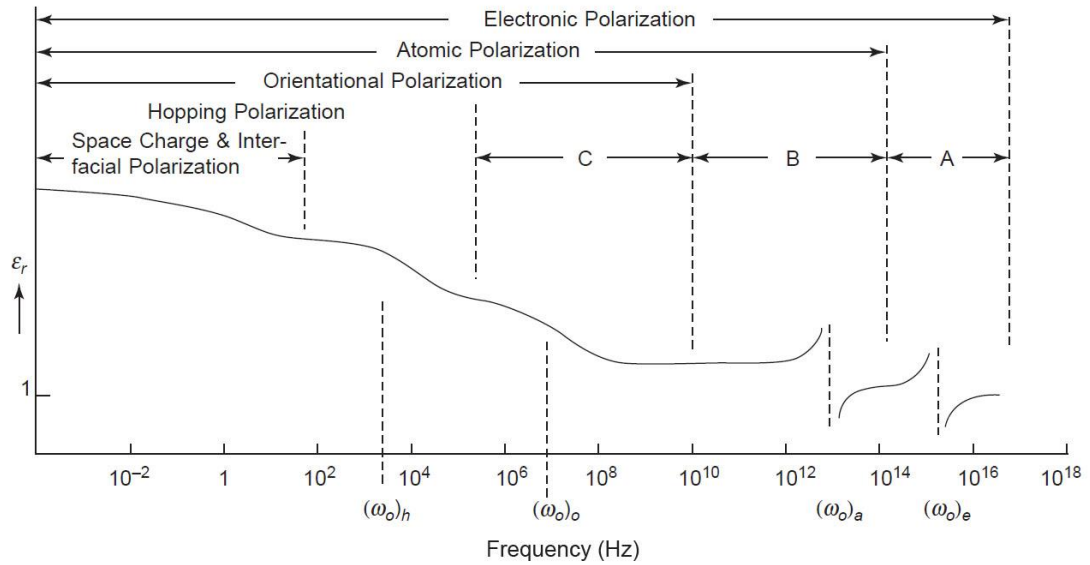


Figure 2.1: The relative permittivity (dielectric constant) as function of frequency (Kao, 2004).

2.3.1 Electronic Polarization

Electrons cloud around the centre of nucleus can be polarized when electrical field is applied. The polarization is known as electronic polarization and occurs in all dielectric materials. The centre of negatively charged electrons cloud is displaced toward the positive direction of the electric field, and the proton is displaced toward the negative direction of the electric field, as shown in Figure 2.2.



Figure 2.2: Electronic polarization that results from the distortion of an atomic electron cloud by an electric field (Wyatt and Dew-Hughes, 1974).

2.3.2 Atomic or Ionic Polarization

Ionic or atomic polarization is only found in ionic materials under electrical field. Cations are displaced toward the electrical field direction and anions displaced toward the opposite direction and net dipole moments are increased. This process is shown in Figure 2.3.

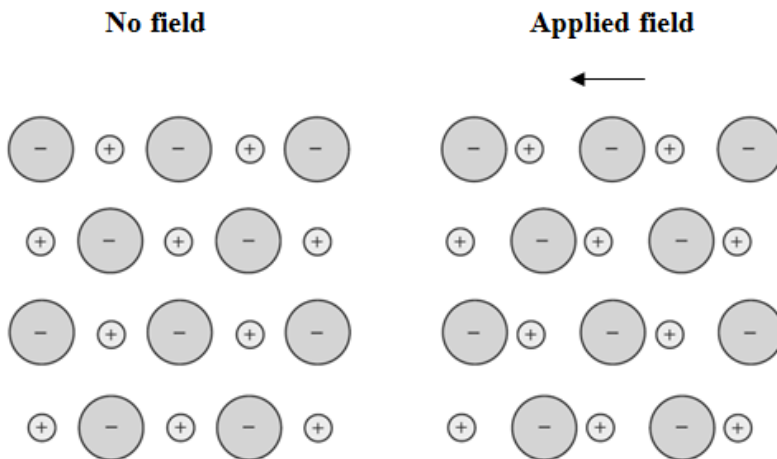


Figure 2.3: Ionic polarization that results from the relative displacements of electrically charged ions in response to an electric field (Wyatt and Dew-Hughes, 1974).

2.3.3 Orientation or Spontaneous Polarization

Orientation polarization or spontaneous polarization is only found in materials that possess permanent dipole moments. Rotation of the permanent moments into the direction of electric field caused the polarization as represented in Figure 2.4. This polarization type strongly depended on temperature where decreasing the temperature will resist the alignment and decrease the polarization.

The alignment process of the permanent dipole required time to perform and in case of AC type of electrical field, the lag between the field and the polarization is

known as dielectric loss and by increasing frequency caused the polarization to totally disappear.



Figure 2.4: Response of permanent electric dipoles (arrows) to an applied electric field, producing orientation polarization (Wyatt and Hughes, 1974).

2.3.4 Interface or Space Charge Polarization

Some amorphous and polycrystalline dielectric materials with grains and grain boundary are also capable to possess space charge polarization. Unlike other polarization, this type of polarization does not come from dipole moment of atom or molecule, but originated from mobile and trapped charge inside the material inhomogeneity like grains or grains boundary or defects of the materials. Figure 2.5 shows an illustration of polycrystalline solids or in materials consisting of traps charge between the grains. According to Moulson & Herbert (2003) and Kao (2004), charge carriers such as electrons, holes, or ions could be injected from electrical contacts and trapped in the bulk or at the interfaces of the contact. The charge carriers could be impeded to be discharged or replaced at the electrical contacts. This can form space charges and the field distribution will be distorted, and hence, the average dielectric constant will be affected.

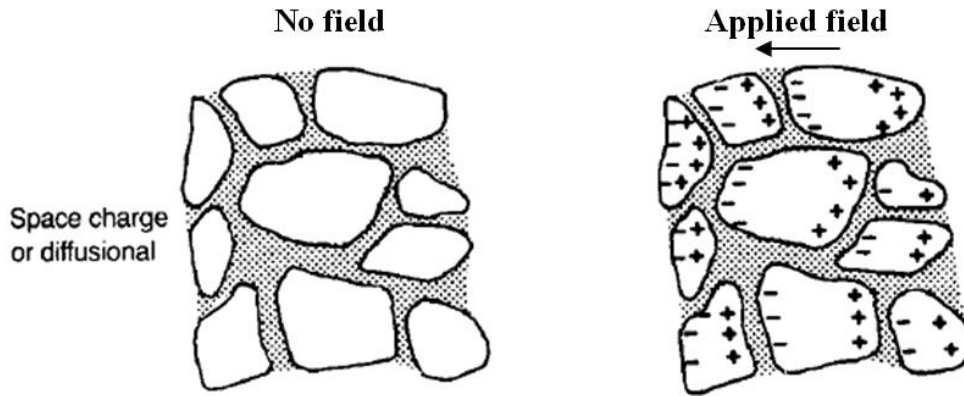


Figure 2.5: Space charge polarization which is caused by trapped charges at polycrystalline material (Moulson and Herbert, 2003).

Interface polarization is a possible mechanism of high dielectric constant of CCTO. CCTO microstructure consists of semiconducting grain and resistive grain boundaries. When the electric field is applied, the trapped negative charges inside the grains are attracted toward the positive terminal and vice versa. The grain boundaries trap the charges from moving and this mechanism is known as internal boundary layer capacitance (IBLC).

2.4 Miniaturization of Electronic Device

The advantage of high dielectric constant ceramic is miniaturisation capability to many electronic device such capacitor, resonator, resistor and oscillator. As an example, this can be understood from the principle mechanisms of working capacitor. Figure 2.6 shows a system of perfect dielectric material under static electric field and undergo polarization process like a capacitor system. The system tends to reduce the potential energy by attracting the piece of materials into the space between the two electrodes. The electrodes consist of two metal plates parallel to each other with area A and a separation of the plate is d . Fringing effect at the edge was ignored first. D_0 is

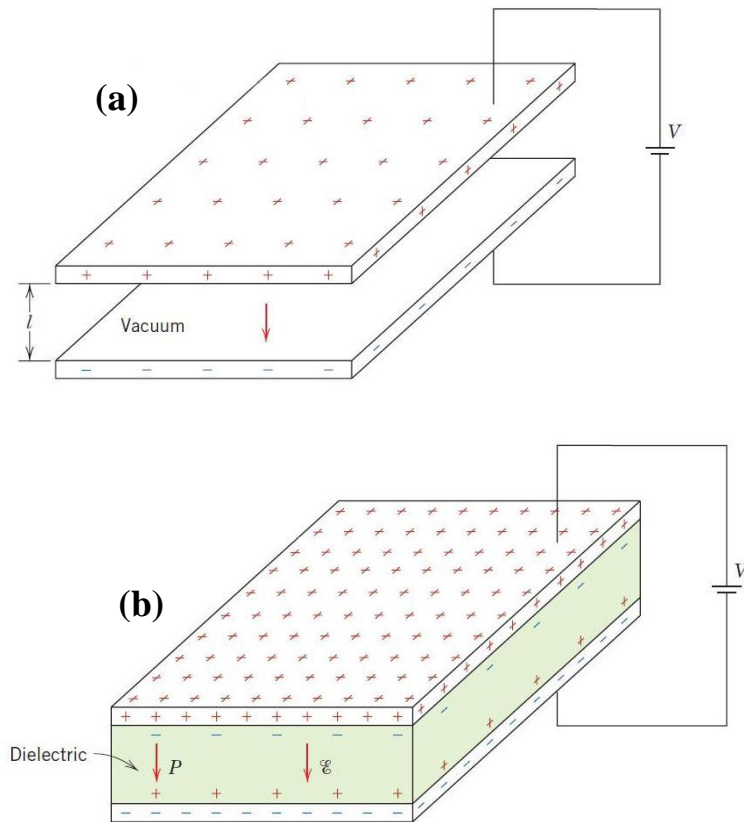


Figure 2.6: A parallel-plate capacitor (a) when a vacuum is present and (b) when a dielectric material is present (Callister and Rethwisch, 2007).

The system was charged to applied electrical field by positive charged ($+Q$) on the upper and on the lower plate were charged with negative charge ($-Q$) at the same magnitude.

This process was done by connecting the electrical power supply source of direct current across the electrodes and charging the system as capacitor. After disconnecting the power source, the charge will remains inside the electrodes. Electrical potential difference (V) was created by the charges or charged electrodes across the d distance and proportional to the value of Q . The relation can be written as

$$V \propto Q \quad (2.1)$$

and

$$V = \frac{Q}{C} \text{ or } Q = CV \quad (2.2)$$

C is the proportionality constant of Q and V known as capacitance. Coulomb's per volts or Farads is the units of capacitance. The surface charge density on the electrode can be expressed as σ_s and the charge Q can be written as Equation (2.3). F is the electric field strength (V/d) and d is the distance between the two electrodes and A is surface area of the individual electrode.

$$Q = C(Fd) = \sigma_s A \quad (2.3)$$

To understand clearer in term of capacitance (C), Equation (2.3) can be expressed such as Equation (2.4) where ϵ is the permittivity of dielectric medium between the two electrodes and have a unit (Farad/meter).

$$C = \frac{Q}{V} = \frac{\sigma_s A}{Fd} = \epsilon \frac{A}{d} \quad (2.4)$$

Because of the permittivity of medium between the two electrodes as shown in Figure 2.6(a) can affect capacitance value, the vacuum medium is taken as a standard. The permittivity ϵ become ϵ_0 and called the permittivity of a vacuum. The permittivity of vacuum is a universal constant having the value of 8.85×10^{-12} F/m. If the dielectric material is inserted into the medium within the electrodes as shown in Figure 2.6(b), then ϵ is the permittivity of the dielectric material. The relative permittivity ϵ_r with no unit as shown in Equation (2.5) is usually known as the

dielectric constant for the dielectric material and the value is equal to the ratio of two permittivity, 1) permittivity of vacuum and 2) permittivity dielectric material).

$$\epsilon_r = \frac{\epsilon}{\epsilon_0} \quad (2.5)$$

In order to identify dielectric constant of the dielectric materials, Equation (2.4) can be merged with Equation (2.5) to become Equation (2.6).

$$\epsilon_r = \frac{dC}{\epsilon_0 A} \quad (2.6)$$

The capacitance (C) value can be measured by using LCR meter, Impedance Spectroscopy or Autolab Potentiostat. If the dielectric constant of dielectric material is already known, the capacitance can be predicted as shown in Equation (2.7). In miniaturization process, the plate area, A is decreased and this will lower the capacitance (Callister and Rethwisch, 2007). To overcome the reduction, dielectric constant ϵ_r should be increased by replacing with high dielectric constant ceramic.

$$C = \frac{\epsilon_r \epsilon_0 A}{d} \quad (2.7)$$

The distance between two electrodes, d can be reduced to increase the capacitance amount. But the decrease of the d is also increasing the electron tunnelling between the electrodes especially when the d achieves a critical distance.

2.5 High Dielectric Constant Ceramic

High dielectric constant ceramic is electroceramic with high dielectric constants. According to Kao (2004), the Electronic Industries Association (EIA) in the United States has specified capacitor from ceramic based into three classes.

Class I is a low dielectric constant materials (15 to 500), also low dielectric losses ($\tan \delta < 0.003$), a low temperature co-fired ceramic (LTCC), and a low aging rate of the capacitance value. The working temperature range is -55 to $+85^{\circ}\text{C}$ (Kao, 2004).

Class II is a medium to large dielectric constant (500 to 20,000) with general properties similar to BaTiO_3 ceramics. The dependence of temperature, electric field, and frequency is stronger than Class 1, and the temperature co-fired ceramic (TCC) value is higher (Kao, 2004).

Class III is the materials possessing conductive phase at the surface of the electrode and this reduces the effective thickness of the dielectric material. The properties are similar to class II but the dielectric breakdown is lower. If the thickness is lower than the critical size, the materials loss dielectric behaviour and electrical tunnelling is higher (Kao, 2004).

Ferroelectric ceramic usually have very high dielectric constant larger than 1000 and very sensitive to temperature, electric field and frequency. Processing parameters also can affect the electrical properties such as synthesis technique, particle size of raw materials, calcination and sintering temperature (Callister and Rethwisch, 2007; Kao, 2004).

Crystalline materials are always grouped according to their crystal structure and the basic arrangement of the atoms will give some basic properties of the materials. One of the essential structures in dielectric material is perovskite structure. This unique structure was initially found in Ural mountain of Russia by Gustav Rose in 1839 and a Russian mineralogist, Perovski was named to the new structure. The compound possessed a structure of ABX_3 . A and B are two different size of cations and X is an anion tied both of the cation together and usually is oxygen or O. ABX_3 structure also shown as ABO_3 . The A sited atoms is usually larger than B sites atoms. The perovskite structure was implemented on many others. Figure 2.7 shows the basic location of ABX_3 atoms in perovskite crystal structure.

Many useful properties of perovskite dielectric material were utilized for into applications. Most of them possess the properties of ferroelectric, piezoelectric, pyroelectric and superconductor (Ye, 2008). Ferroelectric group are usually having very high dielectric constant because of the existence of orientation polarization interior of ceramics grain. Electroceramic materials which have shown the structure of perovskite are like $BaTiO_2$, $MgSiO_3$, $MgTiO_3$, $PbTiO_3$, and $CaTiO_3$ family like CCTO.

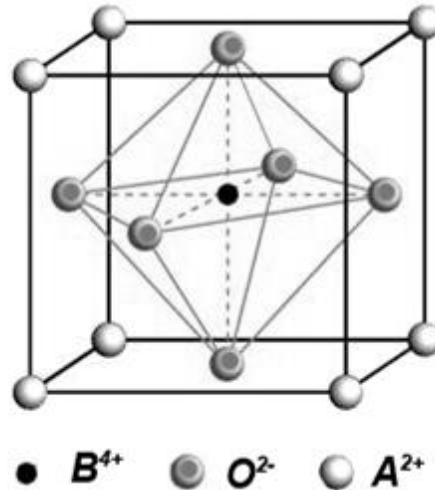


Figure 2.7: Simple cubic structure of perovskite (Howard & Kennedy, 1999)

In the past 50 year, high dielectric constant ceramics such as BaTiO_2 and BaSrTiO_2 are the promising material for electronic application and this was proved when many devices used these materials nowadays. But for further miniaturization process, higher dielectric constant ceramic should be used and this caused on-going research in this field.

In year 2000, a giant dielectric materials known as $\text{CaCu}_3\text{Ti}_4\text{O}_{12}$ was found to possess very high dielectric constant and proposed as promising material for further miniaturizing electronic devices (Subramanian et al., 2000).

2.6 Calcium Copper Titanate ($\text{CaCu}_3\text{Ti}_4\text{O}_{12}$)

Because of unusual dielectric property CCTO received great interest from many researchers (Adams et al., 2002; Homes et al., 2001; Subramanian et al., 2000). CCTO has giant dielectric constant (10^5) and constant at temperature region from 100 to 400 K from low to medium frequency of alternating current (AC) (1 Hz – 1 MHz) (Chakravarty et al., 2007; Ramirez et al., 2000).

CCTO was synthesis by Bochu et al., (1979) and the crystal structure was determined by neutron powder diffraction. Subramanian et al., (2000), Homes et al., (2001) and He et al., (2002) have refined the structure model and unit cell of CCTO. CCTO is perovskite-related body centred cubic (BBC) with the combination of Ca^{2+} cation in the A site and Cu^{2+} cation in the B site while O_3 bonded them together in ABO_3 structure (Figure 2.7). Figure 2.8 describes a unit of CCTO cell with four tilted TiO_6 proveskite-type. According to Homes et al., (2001), the unit cell is based on a cubical shape with A-cation in the centre of the cube, the B-cation in the corner and the anion in the each edge of tilted TiO_6 octahedral. The 6 coordination of the B-cation and 12 A-cation stabilized the structure of CCTO.

CCTO unit cell is grouped to $Im\bar{3}$ space group with a lattice parameter of 7.391 Å. Subramanian et al., (2000) have reported there is no structure change down to 35 K of temperature and the structure is still intact. CCTO shows antiferromagnetic properties at temperature of 25 K which can be explained by the pair of Cu-Cu neighbour has antiparallel spins in the double primitive cells (Mozzati et al., 2003). Antiferromagnetic materials are still magnetic from a behavioural point of view, but they do not produce an external magnetic effect, because the magnetic moments tend to cancel each other.

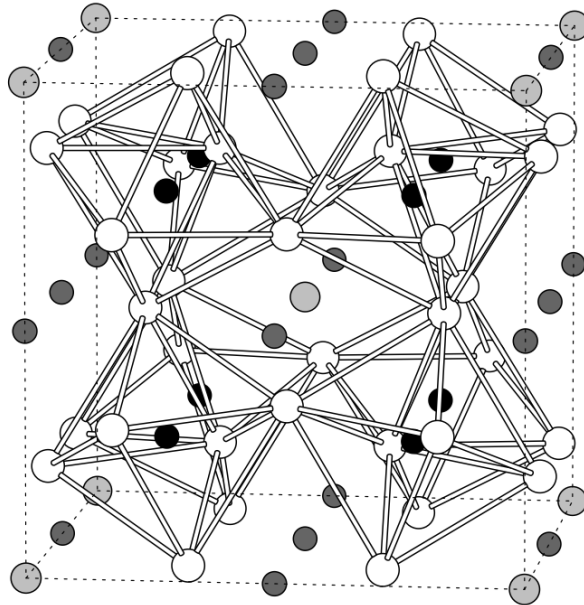


Figure 2.8: Structure of $\text{CaCu}_3\text{Ti}_4\text{O}_{12}$ showing tilted oxygen octahedral. White, light, dark, and black atoms are O, Ca, Cu, and Ti respectively. Dashed lines indicate 40-atom primitive cell of antiferromagnetic spin structure (He et al., 2002).

2.7 Electrode Materials and Surface Layer Effects

Connection of electroceramic to the electrical circuit as a device is very important and this is taken placed by electrodes. Suitable material should be used to produce the best output and usually high conductive metal like gold, silver, aluminium and platinum are the best candidates(Lunkenheimer et al., 2002; Wang and Zhang, 2006). The contact should be studied because several types of contact are possible when the voltage is applied and this depends on the both electrode material and bulk ceramics.

In the case of CCTO, the electrical properties was reported to be sensitive to the contact between the electrode and the CCTO bulk ceramic (B. Shri Prakash and Varma, 2007; Putjuso et al., 2011; Wang and Zhang, 2006; Yang et al., 2005). Wang and Zhang, (2006) reported the contact effect to the CCTO electrical properties was reduced after the samples was polished to remove oxygen vacancies rich site at the

outer surface. They used Ag as electrode material. Yang et al., (2005) tested several materials (Pt, Ag, and Al) as electrodes and found that the dielectric constant is slightly changes with the different contacts in the testing region of 100 Hz and 1MHz. After the heat treatment of the electrode in inert gas (N₂), the changes with the different contact are become significant.

Grains of CCTO ceramic were proved as *n*-type semiconductor by using impedance spectroscopy and x-ray photoelectric spectroscopy (XPS) (Mei et al., 2008; Sinclair et al., 2002) and the contact with metal electrode can create either ohmic or Schottky effect. Schottky effect can cause a barrier with depleting region on CCTO bulk surface (Yang et al., 2005). This is due to the different work function between the electrodes and the semiconductor. Deng et al., (2009) reported the band gap of CCTO is at least 2.5 eV and measurement from XPS identified that oxygen concentration, accompanied by an oxidation of copper from valence +1 to +2, and an oxidation of Ti³⁺ defects to regular Ti⁴⁺. The comparison between the electrical properties and chemical states of CCTO strongly suggested that semiconductivity if CCTO is related to the formation of negative point defects Cu⁺ and Ti³⁺ in the combination with oxygen vacancies.

According to Kao (2004), the ohmic contact between a metal and a semiconductor is a negligibly small impedance compared to the series impedance of the bulk of the semiconductor which relatively large and more significant to consider. This is due to the free carrier density at and in the vicinity of the contact being much greater than that in the bulk of the semiconductor and the contact may act as an accumulation extended from the interface to the inside of the semiconductor.